

Table of Contents

Cover pages and budget summary

Table of contents

Summary of proposal, personnel, and effort

Scientific/technical/management section (15 pages)

1 - Introduction

2 - Mars Ionospheric Observations During Solar Flares

3 - GPS Range Errors

4 - D Region Absorption

5 - Boston University Mars Ionosphere Model

5.1 - Neutral Atmosphere

5.2 - Solar Irradiances

5.3 - Cross-Sections

5.4 - Reaction Rates

5.5 - Models of Photoelectron-Impact Ionization

5.6 - Model Structure

6 - Preliminary Work

7 - Tasks

8 - Computational Requirements

9 - Anticipated Results and Broader Implications

10 - Relevance to NASA Programs and LWS Objectives

11 - Personnel

References

Biographical Sketch for PI Paul Withers

Current and Pending Support for PI Paul Withers

Letter of Commitment from Collaborator Chamberlin

Letter of Commitment from Collaborator Galand

Letter of Commitment from Collaborator Mendillo

Summary of Personnel and Effort

Budget Narrative

Facilities and Equipment

Title: Simulations of the effects of extreme solar flares on technological systems at Mars

Short title: Extreme solar flares at Mars

Summary of proposal:

We propose to simulate the effects of extreme solar flares and other disturbances on the Mars ionosphere in support of the Joint Focus Topic on Extreme Space Weather Events. Such flares will increase plasma densities at relatively low altitudes on timescales of minutes to hours. Ionospheric total electron content will change, affecting the accuracy of GPS-like navigation systems. Radio wave attenuation due to D-region absorption will change, affecting communications systems. GPS range error and radio signal attenuation will be calculated from a suite of ionospheric simulations. Several different flares will be simulated using time-dependent solar irradiances. Solar zenith angle and other model inputs will also be varied to explore parameter space.

Summary of personnel and effort:

Name	Role	Institution	Funded Effort per year	Unfunded Effort per year
Dr. Paul Withers	PI	Boston Univ.	4 months	0
Grad Student	Grad student	Boston Univ.	12 months	0
Dr. Phil Chamberlin	Collaborator	Univ. Colorado	0	As needed
Dr. Marina Galand	Collaborator	Imperial College, London	0	As needed
Prof. Michael Mendillo	Collaborator	Boston Univ.	0	As needed

Simulations of the effects of extreme solar flares on technological systems at Mars

1 - Introduction

We propose to use a Mars ionospheric model with time-dependent solar forcing to investigate the effects of solar flares and other lower ionospheric disturbances on radio navigation and communications systems at Mars. This proposal is submitted to the Joint Focus Topic with Planetary Science: Extreme Space Weather Events in the Solar System.

Solar flares increase plasma densities in the bottomside ionosphere. Propagation of radio waves through the ionosphere is affected by this change. Meteors and cosmic rays also produce plasma at low altitudes. Increases in total electron content cause ranging errors in GPS-like navigation systems. Increases in electron density at low altitudes, where neutral number densities and electron-neutral collision frequencies are high, cause radio wave attenuation that affects communications (D region absorption). These two effects will be numerically simulated in this work to better understand how extreme space weather events at Mars affect technological systems. A range of frequencies will be considered.

We believe that the Boston University Mars Ionosphere Model is the first model of a planetary ionosphere with time-dependent solar forcing. As such, it is the first model able to accurately model the effects of solar flares on another planet's ionosphere. This proposal concentrates on Mars for several reasons: Extensive data are available for model validation, the required model already exists, and Mars is a major focus for NASA's human and robotic spaceflight missions. This will be a "first-cut modeling effort that can contribute towards initiating future more detailed research in this subject area" (page B.7-9, ROSES 2007).

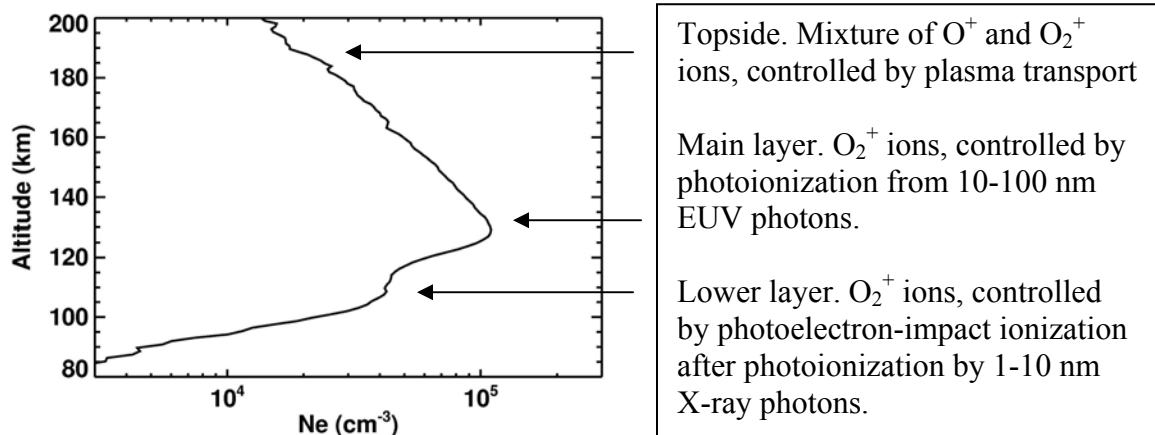


Fig 1. Sample $N_e(z)$ profile from Mars Global Surveyor (MGS).

The Mars ionosphere has a lower layer, a main layer, and a topside (Fig 1; Hanson et al., 1977; Chen et al., 1978). The lower layer has also been called the M1 or E layer and the main layer has also been called the M2 or F1 layer (Fox, 2004; Rishbeth and Mendillo, 2004). The main layer is formed where 10-100 nm EUV photons ionize molecules of CO_2 , the dominant neutral, to produce CO_2^+ ions. These rapidly charge exchange with O atoms, whose mixing ratio is $\sim 1\%$, to form O_2^+ ions. The O_2^+ ions dissociatively

recombine with an electron to form two neutral O atoms. The main layer is controlled by local photochemical processes, not plasma transport, and has a Chapman-like shape. The lower layer is formed where 1-10 nm X-ray photons are absorbed. As these high-energy photons ionize CO₂ to produce CO₂⁺ ions, they eject energetic photoelectrons. These make additional CO₂⁺ ions by “photoelectron-impact ionization” as they thermalize by collisions with CO₂ molecules.

Observations show that lower layer electron densities (Ne) are highly variable on timescales of hours due to variability of 1-10 nm solar irradiance (Fig 2). Since the relative increase in flux during a solar flare is greater at X-ray wavelengths than at EUV wavelengths, the greatest change in the ionosphere during a flare occurs in the lower layer. Photoelectron-impact ionization creates ~5-10 ion-electron pairs per photon absorbed in the lower layer, so this process must be represented accurately in the ionospheric model (Fox, 2004). The photochemical timescale in the ionosphere is proportional to 1/Ne. It is a few minutes at the subsolar main layer and less than an hour for Ne > 1500 cm⁻³ (~100-200 km for solar zenith angles smaller than 80°). The effects of transport processes on the dayside are minor below ~180 km.

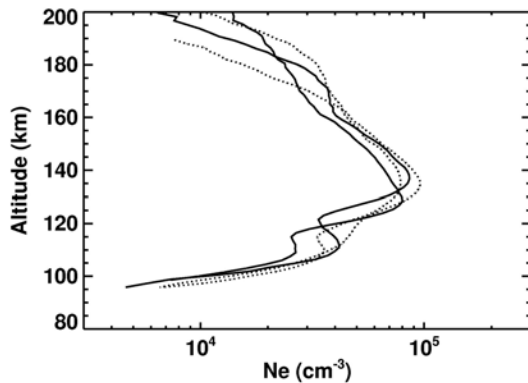


Fig 2. Four MGS profiles showing variability in the shape and size of the lower layer for similar latitude and local solar time.

This proposal describes ionospheric observations during solar flares (Section 2), ionospheric effects on navigation and communications systems (Sections 3-4), model and preliminary work (Sections 5-6), tasks (Section 7), and our work plan (Sections 8-11).

- Our basic research plan is:
- Conduct Mars ionospheric simulations for a range of neutral atmosphere, time-dependent solar irradiances, and solar zenith angles.
 - Calculate radio signal attenuation and GPS range error from these simulations for a range of frequencies and orbiter zenith angles.
 - Investigate trends in the results
 - Study the effects of meteors, <1 nm X-rays, and cosmic rays, which cause low altitude ionization, on radio signal attenuation and GPS range error.
 - Conduct sensitivity studies to determine the robustness of the results.

2 - Mars Ionospheric Observations During Solar Flares

MARSIS (Fig 3; f = 0.1-5.4 MHz) is a topside radar sounder on ESA’s Mars Express spacecraft, which has orbited Mars since 2003. MARSIS often fails to receive a return signal from the Mars surface for periods of days (Morgan et al., 2006; Espley et al., 2007). This has been attributed to absorption of radio waves by ionized plasma far below the main ionospheric layer. The Mars Global Surveyor (MGS) Radio Science (RS) occultation experiment measured 5600 Ne(z) profiles from 1998 to 2006. At least 10

profiles show unusually high Ne in the lower layer at the same time as solar flares were observed from Earth. Two of these have been published (Fig 4; Mendillo et al., 2006).

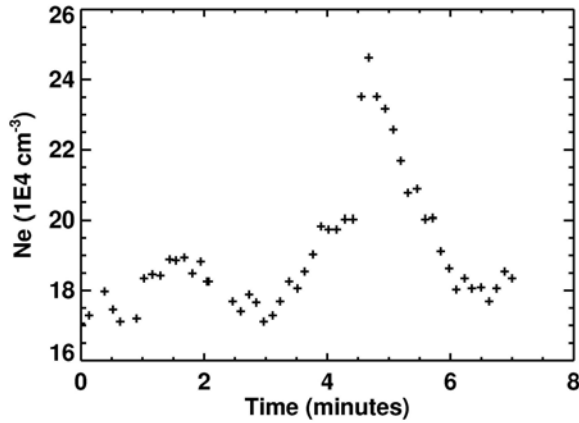


Fig 3. Seven minutes of MARSIS topside radar sounder data at constant solar zenith angle from 15 Sep 2005. Peak Ne increased from $1.8 \times 10^5 \text{ cm}^{-3}$ to $2.4 \times 10^5 \text{ cm}^{-3}$ during an X1.1 solar flare (Gurnett et al., 2005; Nielsen et al., 2006).

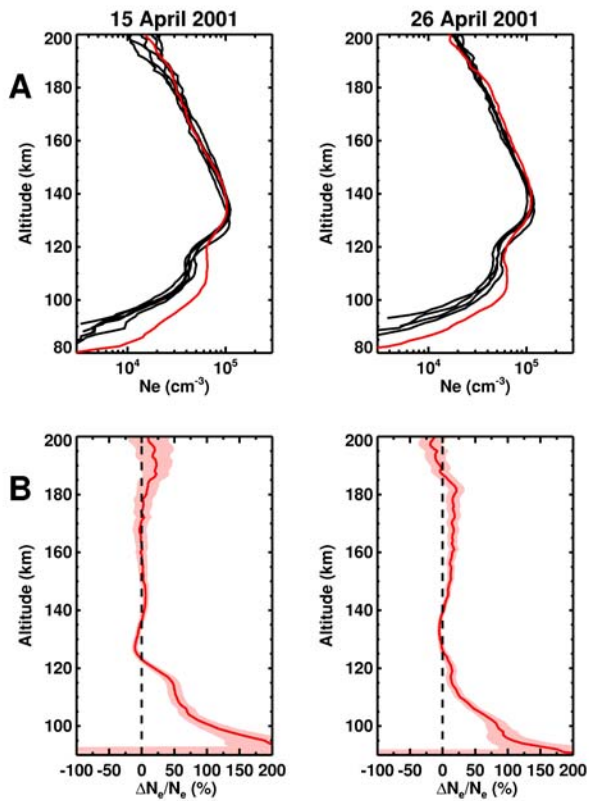
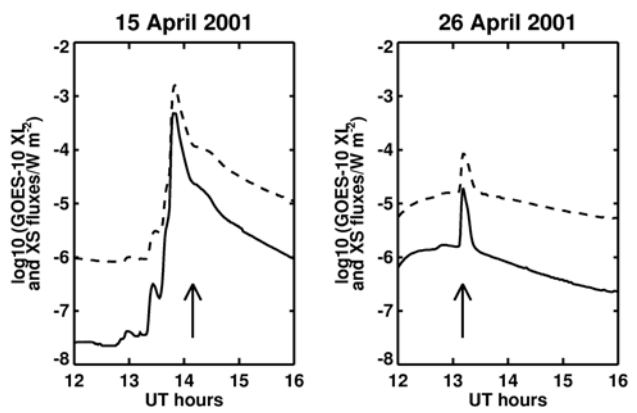


Fig 4. (top) MGS Ne(z) profiles that show increased bottomside Ne during solar flares. (bottom) $\Delta\text{Ne}/\text{Ne}$ versus altitude.

Six Ne(z) profiles were observed at two hour intervals on 15 April 2001. Latitude, solar zenith angle, and local solar time were similar for all six profiles. The first five profiles were very similar, but Ne below 120 km were enhanced in the sixth profile. $\Delta\text{Ne}/\text{Ne}$ increases as altitude decreases, which is consistent with the hardening of the solar spectrum during flares (Fox and Yeager, 2006).

Solar X-ray observations on 15 April 2001 show that photons from the peak of an X14.4 flare reached Mars only 20 minutes before the MGS observation was made (Fig 5). The Earth-Sun-Mars angle was only $\sim 26^\circ$, so both Earth and Mars were exposed to the flare. A similar event occurred on 26 April 2001, when an MGS observation occurred just as photons from the peak of an M7.8 flare reached Mars.

Fig 5. Solar X-ray flux at Earth. GOES XS (solid line, 0.05-0.3 nm) and XL (dashed line, 0.1-0.8 nm) data. Times of MGS Ne(z) are arrowed.



Solar flares have a rise timescale ~minutes and a decay timescale ~hours. The neutral atmospheric responds slowly to increased heating, so ionospheric effects have ceased by the time the neutral atmosphere changes significantly. A model of the ionospheric response to solar flares may use the same neutral atmosphere throughout the simulation.

3 - GPS Range Errors

If radio wave travel time is used to measure the distance between a receiving station (e.g. Mars rover) and a transmitting station (e.g. Mars-orbiting GPS-like satellite), then the measured distance is affected by the presence of the ionosphere between the receiver and the transmitter. Radio waves passing through an ionosphere travel slower than the speed of light and the one-way range error (ΔD) introduced by the ionosphere is given by:

$$\Delta D = 0.403 \frac{TEC_{LOS}}{f^2} \quad (1)$$

where ΔD is in metres, TEC_{LOS} , the line-of-sight total electron content, is in units of 10^{16} electrons m^{-2} , and f , frequency, is in GHz (Mendillo et al., 2004). TEC_{LOS} is given by:

$$TEC_{LOS} = \int Ne \, ds \quad (2)$$

where the integral is performed along the ray path. TEC_{LOS} is related to the vertical total electron content, TEC, by the zenith angle of the orbiting transmitter, OZA:

$$TEC = TEC_{LOS} \sec(OZA) \quad (3)$$

Orbiters in a Mars-based GPS network are likely to be fewer in number than at Earth and likely to perform multiple roles. Existing Mars orbiters use a 400 MHz UHF signal to communicate with landers. This is smaller than terrestrial GPS's ~1.5 GHz frequencies, but could be adapted to a GPS role. NASA may also consider other frequencies.

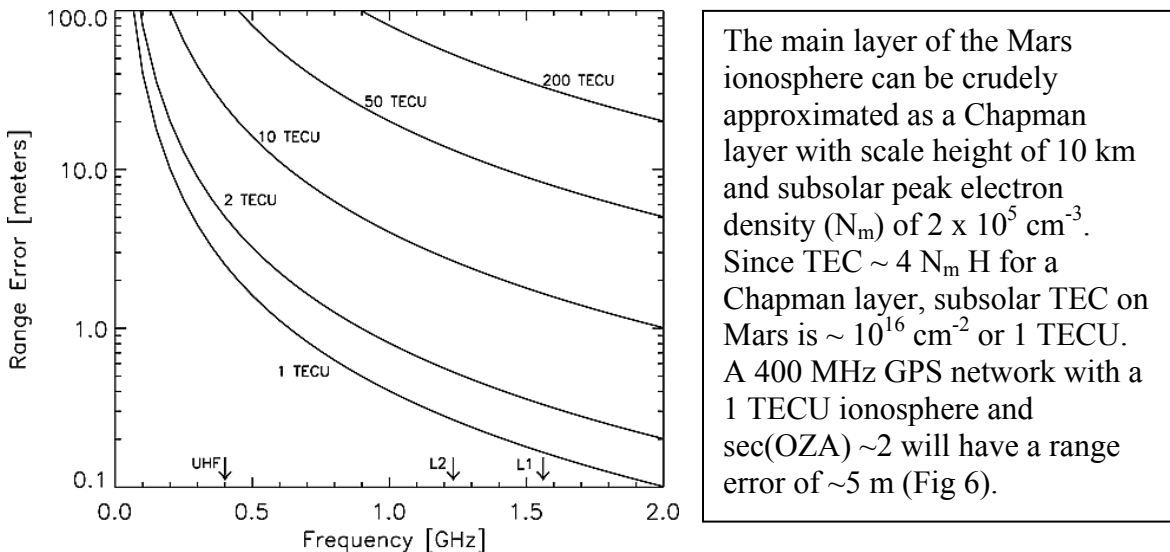


Fig 6. ΔD as a function of frequency and TEC_{LOS} (from Mendillo et al. 2004). 400 MHz UHF and GPS L1, L2 frequencies are marked.

What is the worst-case range error during a large solar flare? This depends on the size of the flare, the flare spectrum, and the details of photoelectron-impact ionization processes

in the Mars ionosphere (Section 1). Predicted ΔD depends on how photoelectron-impact ionization processes are modelled. Doubling of TEC can be seen in our preliminary work (Figure 10b, black dashed line) for an X14.4 flare and it is unlikely that this is the worst possible case. $\sec(OZA) = 2$ is also far from the worst case.

Suppose that a theoretical reference ionospheric model is used to correct for the ionospheric range error under normal solar conditions so that ΔD is affected only by the difference in TEC between the flare-affected ionosphere and the reference ionosphere. Changes in ionospheric range error of ~ 10 m during a large flare for $f=400$ MHz are plausible. ΔD is larger for smaller frequencies. This demonstrates that GPS range errors could be large enough to have significant operational impacts. For example, consider vehicles driving on steep terrain or through a dust storm.

We shall conduct simulations to study the effects of solar flares and other lower ionospheric disturbances on GPS range errors at Mars (Section 7). Relevant frequencies are discussed in Task #1 of Section 7.

4 - D Region Absorption

If E is radio wave amplitude and l is distance, then $K = dE/(E dl)$ is the absorption coefficient per unit length. In the absence of magnetic fields, K satisfies (Rishbeth and Garriott, 1969, Eqn 206):

$$K = \frac{e^2}{2mc\epsilon_0} \frac{Ne}{\mu} \frac{\nu}{(\nu^2 + \omega^2)} \quad (4)$$

where e is the electron charge, m is the electron mass, c is the speed of light, ϵ_0 is the permittivity of free space, Ne is electron number density, ν is the momentum-transfer electron-neutral collision frequency, $\omega=2\pi f$ is the radio wave angular frequency, and μ , the real part of the refractive index, satisfies (Rishbeth and Garriott, 1969, Eqn 204):

$$\mu^2 = 1 - \frac{Ne e^2}{m\epsilon_0\omega^2} \quad (5)$$

ν for electrons and CO_2 is given in Morgan et al. (2006) and Nielsen et al. (2007). The received amplitude, E_r , is related to the transmitted amplitude, E_t , by:

$$\frac{E_r}{E_t} = \exp\left(-\int K dl\right) \quad (6)$$

where dl is along the ray path. If the ray path has zenith angle OZA , then Eqn 6 becomes:

$$\frac{E_r}{E_t} = \left(\exp\left(-\int K dz\right)\right)^{\sec(OZA)} \quad (7)$$

where z is altitude. We label E_r/E_t as the attenuation factor, A .

ν is two orders of magnitude greater in the martian ionosphere than in the terrestrial ionosphere due to the change from N_2 to CO_2 composition (Nielsen et al., 2007). The main layer of the subsolar ionosphere can be crudely approximated as a Chapman layer with $N_m = 2 \times 10^5 \text{ cm}^{-3}$, $H = 10$ km, and $z_0 = 110$ km (Hantsch and Bauer, 1990). Fig 7 shows $K(z)$. A is 0.10 at 5 MHz and 0.98 at 50 MHz for $OZA=0^\circ$. Solar flares, meteors,

solar energetic particles, and cosmic rays can all cause enhanced electron densities below the main ionospheric peak. If Ne between 60 km and 70 km is somehow increased to 10^4 cm^{-3} , then A is $<10^{-4}$ at 5 MHz and 0.87 at 50 MHz. The $\nu / (\nu^2 + \omega^2)$ term in Eqn 7 is crucial. At high altitudes, where $\omega \gg \nu$, large values of Ne do not cause significant attenuation. At lower altitudes, where $\omega \sim \nu$, even small values of Ne can cause significant attenuation. $\omega = \nu$ at 60 km for $f=5$ MHz and at 45 km for $f=50$ MHz.

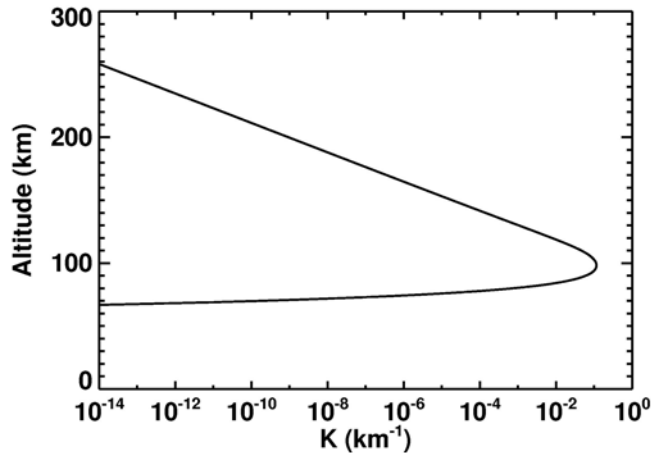


Fig 7. $K(z)$ for $f=5$ MHz.

The electron gyrofrequency is much smaller than the transmitted frequency for $f > 1$ MHz and $B < 100$ nT, so martian crustal magnetic fields have no effect on radio wave attenuation (Rishbeth and Garriott, 1969, Eqn 206).

We shall conduct simulations to study the effects of solar flares and other lower ionospheric disturbances on radio wave attenuation at Mars (Section 7). Relevant frequencies are discussed in Task #1 of Section 7.

5 - Boston University Mars Ionosphere Model

Boston University has developed a 1-D photochemical model of the Mars ionosphere (Martinis et al., 2003; Mendillo et al., 2003; Withers and Mendillo, 2005; Mendillo and Withers, 2006; Withers et al., 2007). Time-dependent solar forcing is a relatively recent addition to the model; results have been presented at conferences (Withers et al., 2007a, 2007b). The main model inputs are neutral atmosphere, solar irradiance, absorption and ionization cross-sections, reaction rates, and a model for photoelectron-impact ionization.

5.1 - Neutral Atmosphere

The current 1-D model spans 80-400 km with 1 km vertical resolution. Neutral species include CO_2 , O, O_2 , N_2 , CO, Ar, NO, H_2 , H, and He. Number densities of major species for two baseline atmospheres (solar maximum and minimum) come from Bougher's Mars Thermospheric General Circulation Model, as published in Fox et al. (1996). Number densities of minor species were provided by Andrew Nagy (personal communication, 2003). There are insufficient data on the Mars upper atmosphere to support a detailed empirical model like MSIS. The neutral atmosphere will be extended to lower altitudes as needed using the same chemical composition as at 80 km and temperatures from models/observations. This will ensure that the flux of ionizing photons out of the bottom of the model is zero.

5.2 - Solar Irradiances

The model has two possible sources of solar irradiances, the well-known Solar2000 model and the Flare Irradiance Spectral Model (FISM). Both are empirical models based on observations from Earth orbit. We discuss the Solar2000 model first. The spectral range of the Solar2000 model is 1.86 - 105 nm and there are 39 spectral bins (a mixture of regions ~5 nm wide and narrow lines) (Tobiska et al., 2003; Tobiska, 2004). The shortest wavelength bins, which will be important in this work, are 1.86-2.95 nm, 3.00-4.92 nm, and 5.05-10.00 nm. Solar2000 outputs one solar spectrum at Earth each day.

FISM outputs solar irradiance at Earth from 0.5 to 195.5 nm with 1 nm spectral resolution and 1 minute temporal resolution (Chamberlin et al., 2004; Chamberlin, 2005; Chamberlin et al., 2005a, 2005b; Chamberlin et al., 2007). It is an empirical model that uses reference solar spectra and data from Earth-orbiting satellites.

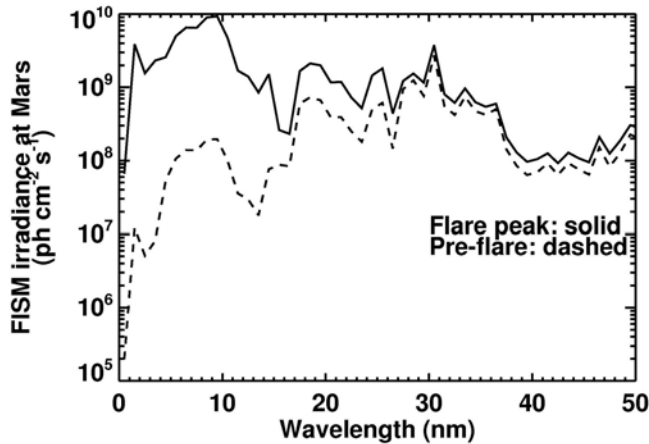


Fig 8. FISM irradiances for 15 April 2001.

FISM data sources include:
(A) GOES, 0.05-0.3 nm and 0.1-0.8 nm, 1980s-present,
(B) TIMED SEE, 27-194 nm at 0.4 nm resolution and nine overlapping bands from 0.1-20 nm at ~5 nm resolution, 2002-present,
(C) SOHO SEM, 26-34 nm and 0.1-50 nm, 1995-present,
(D) SNOE SXP, 2-7 nm, 6-19 nm, and 17-20 nm, 1997-2003, and
(E) SOLSTICE instrument on UARS and SORCE, 120-420 nm at 0.5 nm resolution, 1991-present.

We will primarily use FISM solar spectra in this work, because they have better temporal and spectral resolution than Solar2000 spectra. They will be scaled by $1/R^2$ to account for the different heliocentric distances of Earth and Mars. FISM results are publicly available at ftp://aspftp.colorado.edu/pub/SEE_Data/fism/ (Fig 8). Collaborator Chamberlin will ensure that FISM output for the dates of interest are online, and provide guidance on their use and interpretation.

5.3 - Cross-Sections

Absorption and ionization cross-sections for reactions like $\text{CO}_2 + h\nu \rightarrow \text{CO}_2^+ + e$ should come from a standard source (Schunk and Nagy, 2000). This tabulation matches 37 of Solar2000's 39 wavelength bins, but not the 1.86-2.95 nm and 3.00-4.92 nm bins. Cross-sections for these bins can be calculated using analytic expressions (Verner and Yakovlev, 1995; Verner et al., 1996). However, the three shortest wavelength bins in the Solar2000 spectra (1.86-2.95 nm, 3.00-4.92 nm, 5.05-10.00 nm) are too broad for our purposes. Cross-sections vary significantly with wavelength in the 1-10 nm range (Fig 9 and Fox (2004, Fig 12)). This wavelength range controls photoionization in the lower layer. The underlying physical reason for the abrupt increase in cross-section with

decreasing wavelength is that photons have sufficient energy to eject electrons from the inner electron shells as well as just the outer shell. Cross-sections for molecules are the sum of the cross-sections of the constituent atoms at these wavelengths (Fox et al., 2004). Almost all photons shorter than 20 nm ionize a neutral when they are absorbed, whereas lower-energy photons can be absorbed without ionization.

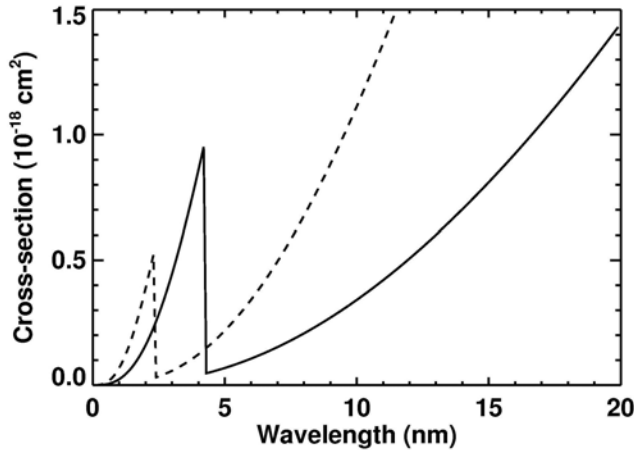


Fig 9. Theoretical ionization cross-sections for C (solid) and O (dashed) (Verner and Yakovlev, 1995; Verner et al., 1996). The cross-section for CO₂ is the sum of those for its constituent atoms at these wavelengths ($\sigma_{\text{CO}_2} = \sigma_{\text{C}} + 2\sigma_{\text{O}}$). Laboratory data for CO₂ with the appropriate spectral range and resolution are not available.

We require cross-sections with high spectral resolution in the 1-10 nm range, but the analytic expressions that can calculate them are invalid for molecules (e.g. CO₂) at long wavelengths. We solve this problem as follows.

We use the 0.5 nm, 1.5 nm, ..., 9.5 nm FISM irradiances and generate cross-sections for these wavelengths using the analytical expressions of Verner and Yakovlev (1995) and Verner et al. (1996). These expressions, which rely on molecular cross-sections equaling the sum of the constituent atomic cross-sections, are inaccurate at long wavelengths, so they cannot be used at all FISM wavelengths. We assign the remaining FISM wavelengths to their closest Solar2000 spectral bins and use the usual cross-sections from Schunk and Nagy (2000). Thus we have a composite set of 46 wavelengths for the spectrum and cross-sections. High spectral resolution is used for 10 short wavelengths, where it is needed (Fig 9) and where Verner's cross-section expressions are valid. Standard Solar2000 wavelength bins are used at 36 longer wavelengths to match the available cross-sections. FISM wavelengths >105 nm, longward of the last Solar2000 bin, are neglected because they do not produce ions in the Mars ionosphere. Lyman B 102.6 nm photons, which ionize O₂ in the terrestrial atmosphere, do not produce ions on Mars. The model was first developed with time-independent solar forcing from a 39 wavelength Solar2000 spectrum.

5.4 - Reaction Rates

Ions may undergo chemical reactions before being lost by neutralization. Rate coefficients for reactions like $\text{CO}_2^+ + \text{O} \rightarrow \text{O}_2^+ + \text{CO}$ and $\text{O}_2^+ + \text{e} \rightarrow \text{O} + \text{O}$ are taken from a standard source (Schunk and Nagy, 2000). Some rate coefficients depend weakly on electron temperature (Hansen and Mantas, 1988; Choi et al., 1998).

5.5 - Models of Photoelectron-Impact Ionization

Photoelectron-impact ionization creates ~5-10 ions per photon absorbed in the lower layer (Fox et al., 1996; Fox, 2004). This process must be modelled accurately for the ionospheric model to realistically respond to a solar flare. It is possible to model the energy and trajectory of a photoelectron as it thermalizes by collisions with neutral molecules, tracking how many molecules are ionized in these collisions. Photoelectron collision models have been used in certain terrestrial ionospheric models (e.g. Lummerzheim and Lilensten, 1994; Brelly et al., 1996; and references therein) and in some Venus and Mars ionospheric models (e.g. Kim et al., 1989; Fox, 2004).

However, many terrestrial ionospheric models use a simple scaling factor to represent all photoelectron-impact ionization processes (e.g. Richards and Torr, 1988; Lilensten et al., 1989; Titheridge, 1996). The photoelectron efficiency or primary efficiency, R , is the ratio of the number of ions produced by photoelectron-impact ionization (P_i^{EI} , hard to model) to the number of ions produced by photoionization (P_i^P , easy to model). If R is known, then photoelectron-impact ionization can be modeled as a simple multiplying factor and P_i^{EI} in Eqn 1 (below) can be replaced by $R \times P_i^P$. This simplifies the model and, as long as R is chosen correctly, does not impact the model's accuracy.

There are many models of R for the terrestrial ionosphere (e.g. Rees and Jones, 1973; Richards and Torr, 1988; Lilensten et al., 1989; Titheridge, 1996). We shall investigate how the following three parameterizations affect the simulated Mars ionospheric electron density profile, GPS range error, and D region absorption.

(A) The Rees and Jones (1973) parameterization for Earth is that an ion-electron pair is created for every 35 eV difference between the energy of the ionizing photon and the neutral species's ionization potential. The ion-electron pair is produced locally, at the same altitude as the photon is absorbed.

(B) Titheridge (1996) used models of electron collisions to determine R as a function of wavelength and ion species for Earth. Values in his Table 3 approximately satisfy $R=12 \exp(-\lambda / 7 \text{ nm})$ and do not vary much by species (O^+ , O_2^+ , N_2^+).

(C) Fox (2004) has developed a Mars ionosphere model that included electron collisions and electron-impact ionization. The effective R parameterization can be seen in several figures as a function of altitude for different simulations (Fox et al., 1996; Fox and Yeager, 2006). Despite its sophistication, this model's simulations reproduce lower layer observations relatively poorly. The solar irradiances used by Fox (2004) may be inaccurate at short wavelengths.

Clearly, the study of photoelectron-impact ionization processes on Mars is not as accurate as it is on Earth. These uncertainties are not a fatal problem. As requested by the NRA, this proposal provides "first-cut modeling efforts that can contribute toward initiating future more detailed studies in this subject area." Collaborator Galand will ensure that

reasonable R parameterizations are used (Galand et al., 1997, 1999, 2006). Extensive Mars Ne(z) data are available as a sanity check for our simulated ionospheric profiles.

5.6 - Model Structure

For completeness, we now discuss the underlying structure of the model.

$$\frac{dN_i}{dt} = (P_i^P + P_i^{EI} + P_i^C) - (L_i^C + L_i^{DR}) \quad (1)$$

This is the continuity equation for ion species I^+ , as represented by the index i . N_i is the number density of I^+ , t is time, P_i^P is the rate of production of I^+ by photoionization, P_i^{EI} is the rate of production of I^+ by photoelectron-impact ionization, P_i^C is the rate of production of I^+ by charge exchange reactions, L_i^C is the rate of loss of I^+ by charge exchange reactions, and L_i^{DR} is the rate of loss of I^+ by dissociative recombination reactions. Upper case N refers to ion/electron densities, lower case n to neutral densities. Four of the five terms on the right-hand side of Eqn 1 are as follows; P_i^{EI} is replaced by $R \times P_i^P$ as discussed in Section 5.5.

$$L_i^{DR} = \alpha_i N_i N_e \quad (2)$$

L_i^{DR} is the rate of loss of I^+ in the reaction $I^+ + e \rightarrow$ neutral products (e.g. $O_2^+ + e \rightarrow O + O$), and α_i is the relevant rate coefficient. Only molecules can dissociatively recombine.

$$L_i^C = \sum_{s,j,r} k_{isjr} N_i n_s \quad (3)$$

L_i^C is the rate of loss of I^+ in the reaction $I^+ + S \rightarrow J^+ + R$, k_{isjr} is the relevant rate coefficient, and n_s is the number density of neutral species S .

$$P_i^C = \sum_{j,r,s} k_{jris} N_j n_r \quad (4)$$

P_i^C is the rate of production of I^+ in the reaction $J^+ + R \rightarrow I^+ + S$ and k_{jris} is the relevant rate coefficient.

$$P_i^P = \sum_{r,\lambda} \sigma_{ion,i,r}(\lambda) n_r(z) F(z, \lambda) \quad (5)$$

P_i^P is the rate of production of I^+ in the reaction $R + h\nu \rightarrow I^+ + e$, $\sigma_{ion,i,r}$ is the relevant wavelength-dependent ionization cross-section, and F is the flux (photons $cm^{-2} s^{-1}$) at that altitude (z) and wavelength (λ). F is given by:

$$F(z, \lambda) = F_0(\lambda) \exp(-\tau(z, \lambda)) \quad (6)$$

F_0 is the value of F at the top of the atmosphere and τ is wavelength-dependent optical depth, which is given by:

$$\tau(z, \lambda) = \sum_r \frac{1}{\cos(SZA)} \int_{z'=z}^{z'=\infty} n_r(z') \sigma_{abs,r}(\lambda) dz' \quad (7)$$

SZA is solar zenith angle and $\sigma_{abs,r}$ is the relevant wavelength-dependent absorption cross-section. A more accurate calculation of optical depth is used near the terminator.

There are no spatial derivatives, and therefore no boundary conditions, because plasma transport is not modeled here. Initial conditions are irrelevant because the model is spun-

up over several Mars days, which is much longer than the <1 hour dayside photochemical timescale at the main and lower layers.

6 - Preliminary Work

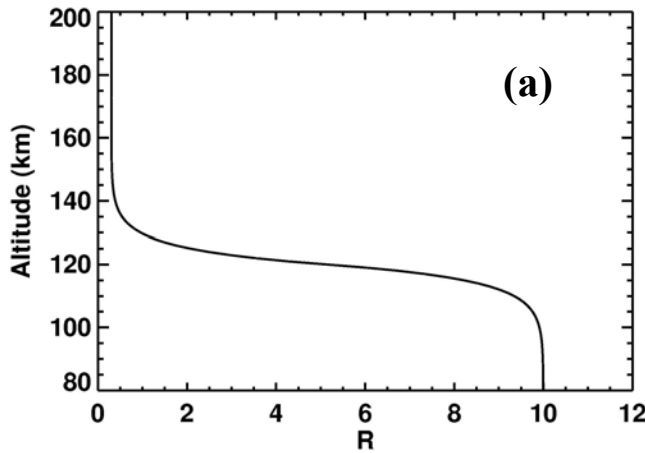
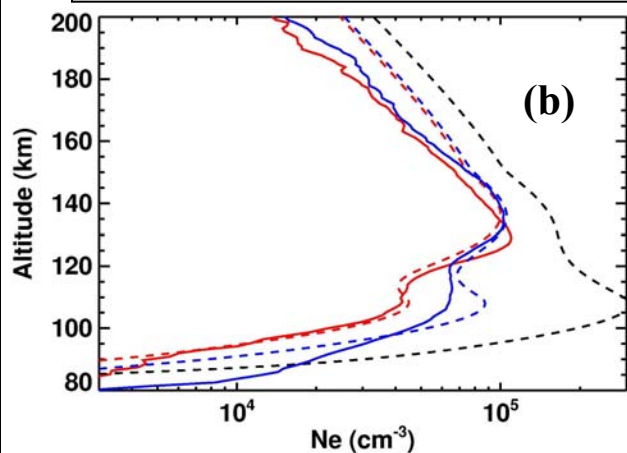


Fig 10b. The red pre-flare simulation almost matches the shape of the observed lower layer and accurately predicts Ne below 95 km. The blue simulation poorly matches the shape of the lower layer and underpredicts Ne below 95 km. This altitude-dependent model for R shown in Fig 10a works for one case, but not the other. A wavelength-dependent expression for R might be successful in both cases (Section 5.5), because the average wavelength of ionizing photons at a given altitude is shorter during the flare (blue) than before the flare (red).

Fig 10a. A simple R(z) was used for this demonstration. It is consistent with Fox et al. (1996). We have performed three simulations for the 15 April 2001 MGS RS observations using solar irradiances that do not vary with time (Fig 10b). The first case (red) uses irradiances before the flare, the second (black) uses irradiances at the peak of the flare, and the third (blue) uses irradiances from the time of the MGS observation with a large lower layer. Observations are solid lines, simulations are dashed lines. Ne in the lower layer exceed those in the main layer for the “flare peak” simulation, which is unusual.



7 - Tasks

We shall perform numerical simulations of ionospheric structure during solar flares and other disturbances and investigate how A and ΔD change during each simulation. A and ΔD have a simple functional dependence on the zenith angle of the orbiter with respect to the lander, OZA. ΔD has a simple functional dependence on radio frequency, but A has a complex dependence on radio frequency.

How strong does a flare have to be to have significant effects on technological systems? How long do those effects last? What are the effects of cosmic rays and meteors? What frequencies are most affected? Are the results significantly different from terrestrial experience? If so, why? How reliable are our results? Motivated by these questions, we will perform the following tasks.

Task #1: Current Mars missions use 400 MHz for short-range communications between spacecraft and ~5 GHz for communications to Earth. Sections 3 and 4 showed that ionospheric effects on ΔD , but not A , can be significant at $f > 400$ MHz. Future Mars missions may use smaller frequencies for some navigation/communication needs, as aircraft (10s of MHz) and hand-held systems (46 MHz cordless phones) on Earth do today. The dependence of A on frequency in the 1 MHz - 10 GHz range will be studied using observed $N_e(z)$ profiles and the preliminary simulations (Fig 10b). Results will be used to select a small number of frequencies to use in the subsequent Tasks.

Task #2: A and ΔD depend on the model's neutral atmosphere, parameterization for R , time-dependent solar flare spectrum, and the solar zenith angle. In this task we shall conduct many simulations to fully cover the available parameter space. Five different neutral atmospheres will be used (solar maximum/minimum, winter/summer hemisphere, plus one case during a global dust storm). Three parameterizations for R will be used (Section 5.5). Four different solar flares will be used, two moderate flares and two large flares. They may include flares that had significant effects at Earth, flares that affected MGS $N_e(z)$ profiles, or other flares of interest to our Focused Science Team. Seven solar zenith angles of 0° , 15° , 30° , 45° , 60° , 75° , and 85° at the time of the flare peak will be used. Equatorial latitudes will be used so that SZA does not vary a lot during the flare. $5 \times 3 \times 4 \times 7$ corresponds to 420 simulations.

A pre-defined initial analysis plan is necessary to efficiently identify the magnitude of the effects, trends, and interesting features.

- Orbiter zenith angle of 0° will be used to find the A and ΔD at the time of the flare peak for each of the 420 simulations. We shall determine whether A and ΔD vary significantly with the neutral atmosphere, R parameterization, solar flare, and SZA, then characterize any apparent trends in the 420 values of A and ΔD . A small subset of typical simulations will be selected based on these results.
- The dependence of A and ΔD on time will be studied in the subset of typical simulations. Do they decay exponentially or in some other way? What is the timescale? Once manual inspection of the subset of simulations has led to the formulation of specific quantitative questions that can be automated, the entire set of simulations will be studied.
- We shall quantify how the three different R parameterizations affect the simulated electron densities, A , and ΔD . If they cause major differences, then we shall compare simulations and observations to identify and improve the best R parameterization.
- Do values of A and ΔD at the flare peak have a clear dependence on SZA? If so, do other properties, such as timescale for changes in A and ΔD or the effects of radio frequency, also have clear dependences on SZA? Can these trends be explained in terms of basic physical processes?

Task #3: Additional simulations will be performed as sensitivity studies. The magnitude of uncertainties in the neutral atmosphere, the cross-sections, R parameterizations, and the solar flare spectrum will be estimated. Small changes will be made to these model inputs and simulation results will then be analysed to determine how A and ΔD are affected by these changes. This will be used to provide an estimate of the uncertainty in values of A and ΔD in the other Tasks.

Task #4: A plasma layer due to meteors is sporadically observed in the Mars ionosphere (Patzold et al., 2005). This layer (peak density 6000 electrons cm^{-3} , thickness 10 km, altitude 90 km) will be added to a set of simulated electron density profiles. The effects on A and ΔD of this layer will be determined. Layer properties will then be varied, consistent with observations and theoretical predictions (Pesnell and Grebowsky, 2000; Molina-Cuberos et al., 2003).

Task #5: We shall study whether photons with $\lambda < 1$ nm have significant effects on A and ΔD . FISM's shortest wavelength is 0.5 nm, where $\sigma_{\text{CO}_2} = 2.3 \times 10^{-20} \text{ cm}^2$. At 0.1 nm, σ_{CO_2} is 130 times smaller and photons penetrate an additional five scale heights or 50 km deeper into the atmosphere. Plasma at low altitudes can have large effects on A even if plasma densities are low. Effects on ΔD , which is proportional to TEC, will be smaller. We shall adapt the ionospheric model to include more short wavelength bins, using cross-sections from Verner and Yakovlev (1995) and Verner et al., (1996). Solar irradiances will be obtained from various solar X-ray observations, such as rocket flights and GOES (0.05 - 0.3 nm, 0.1 - 0.8 nm bands) satellites. Composite solar spectra will be constructed from multiple data sources, if necessary, and a time-independent solar spectrum will be used if, as is likely, short wavelength X-ray irradiances are not available with high time resolution. A small number of simulations will be performed at different solar zenith angles, but the neutral atmosphere and R parameterization will be fixed.

Task #6: Cosmic rays, which are not included in most Mars ionospheric models, have been predicted to produce ions at all altitudes. Electron densities of 100 cm^{-3} have been predicted from 30 to 50 km (Fig 11). We shall form composite electron density profiles from the surface to exosphere by adding low altitude electron densities from Fig 11 to our simulated high-altitude electron density profiles. The effects of low altitude plasma on A and ΔD will then be determined. Additional low altitude Ne(z) predictions for different conditions or by other models will also be tested (e.g. Whitten et al., 1971).

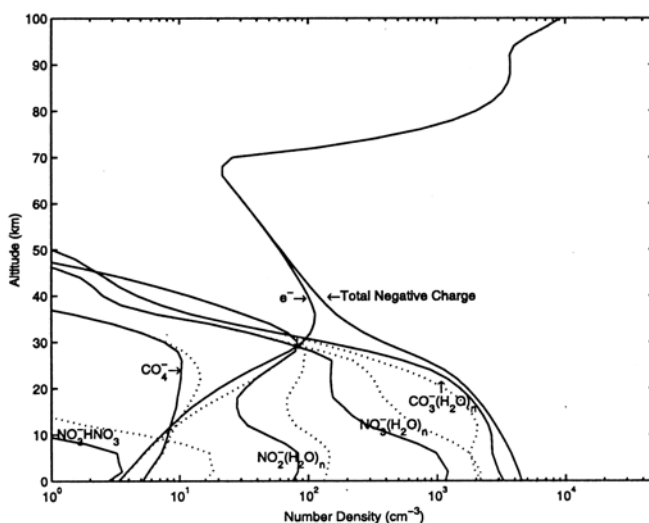


Fig 11. Number densities of electrons and negative ions in the lower Mars ionosphere. Wet case (solid lines) and dry case (dashed lines). From Molina-Cuberos et al. (2002).

No measurements capable of detecting low altitude plasma have been made at Mars. However, the failure of MARSIS to receive radar signals reflected from the Mars surface after major solar energetic particle events suggests that low altitude plasma does exist (Morgan et al., 2006; Espley et al., 2007).

Task #7: Although solar flares are often characterized by a single number that corresponds to their peak irradiance in the 0.1-0.8 nm band, flares with the same classification can have different spectra and time histories. We shall identify ten solar flares with the same (or similar) classifications (hea-www.harvard.edu/trace/flare_catalog) and use them in ionospheric simulations. We shall determine how the results for A and ΔD differ between the different flares.

8 - Computational Requirements

Each simulation takes ~1 hour to run. Task #2 is the most computationally intensive, with 420 simulations. The remaining Tasks will contribute no more than 500 simulations, giving a total of <1000 simulations. The only output that must be stored for each simulation is Ne(z) at 1 minute resolution for a few hours, which isn't a storage problem.

9 - Anticipated Results and Broader Implications

We expect that this effort will lead to the identification of a range of radio frequencies that are not affected by worst-case ionospheric conditions and a range of radio frequencies that are severely affected by worst-case ionospheric conditions. For those frequencies that do experience GPS range error or attenuation, the dependence of A and ΔD on neutral atmospheric conditions, SZA, flare intensity and duration will be quantified. The effects of meteors, <1 nm X-rays, and cosmic rays on A and ΔD will also be investigated. Results and trends will be compared to Earth and we shall seek physical explanations (e.g. N₂ vs. CO₂ composition, magnetic fields) for observed similarities or differences. Collaborator Mendillo has extensive experience in terrestrial aeronomy.

Space weather, including solar flares, affects GPS and communications on Earth so much that the Air Force plans to launch a dedicated satellite (CNOFS) to study their effects (LWS TRT SDT, 2003; LWS TRT Town Hall Meeting Report, 2006). This work will be a step towards characterizing these effects on Mars. Radio propagation through the Mars ionosphere will affect implementation of navigation/communication systems for human exploration. The MARSIS topside radar sounder (Section 2) has already demonstrated that D-region absorption occurs at Mars and prevents radio wave propagation.

10 - Relevance to NASA Programs and LWS Objectives

This effort addresses NASA Strategic Sub-goals 3B and 3C (Table 1 of the ROSES NRA). This effort is directly related to the scientific objectives of the 2011 Mars Scout orbiter - escape processes and the upper atmospheric reservoir available for escape.

This effort will provide the first estimates of how space weather events will degrade or disable communications and navigation infrastructure at Mars. It is a first step towards similar studies for all solar system bodies. It will lead to a better understanding of the hazards present as humans explore space, especially Mars. By the end of Year 1, we will provide preliminary estimates of the frequencies at which values of A and ΔD have significant operational impacts (Task #1) and detailed analyses of how values and time-

history of A and ΔD depend on flare intensity, neutral atmosphere, SZA, and OZA (Task #2). By the end of Year 2, we will have characterized the robustness of our results (Task #3) and determined whether <1 nm photons and meteors affect A and ΔD (Tasks #4, #5). By the end of Year 3, we will have determined whether plasma produced at 30-50 km by cosmic rays affects A and ΔD (Task #6) and determined whether all flares of the same class have the same effects on A and ΔD .

Year 1: Tasks #1, #2

Year 2: Tasks #3, #4, #5

Year 3: Tasks #6, #7

Graduate Student will perform the simulations. Results will be analysed by Withers and Graduate Student. More detailed success measures and deliverables for the “Extreme Space Weather Events” Focused Science Team will be developed with the LWS Program Scientist, Team Coordinator, and other team members once selected team proposals have been structured into an integrated research program, as outlined in page B.7-4 of ROSES (2007).

Cross-disciplinary proposals are solicited by the proposed LWS Decadal Strategic Plan (LWS, 2007). This proposal will stimulate collaboration of planetary scientists and experts in terrestrial aeronomy with the heliophysics community. LWS Strategic Goal 1 concerns accurate modelling of the solar spectrum and its effects on Mars (LWS, 2007). LWS Strategic Goal 4 concerns GPS position error and radio blackouts (LWS, 2007).

11 - Personnel

Principal Investigator Paul Withers will serve as leader of this effort. He has worked extensively on the Mars neutral atmosphere and ionosphere. Recent projects include a study of the relationship between variability in the Sun’s EUV flux due to its 27 day rotation and Mars Ne(z), analysis of Mars ionospheric observations during a solar flare, and the use and development of this Mars ionospheric model (Withers et al., 2003, 2005, 2007a, 2007b; Withers and Mendillo, 2006). His funded effort will be 4 months per year. Support for this proposal would introduce Withers, a young planetary scientist, to the heliophysics community.

The Boston University Astronomy Dept’s PhD program has >40 graduate students. ~ 8 students typically arrive each year. 12 months funding per year for a graduate student is requested. We expect that a 1st/2nd year graduate student will start work on this project. Collaborator Phil Chamberlain (University of Colorado) will ensure that FISM results are available for dates of interest. He will also advise on the general topic of <10 nm solar irradiance. Collaborator Marina Galand (Imperial College, London) will ensure that we use reasonable functions for photoelectron-impact parameterization. She will also advise on the physical significance of the parameters. Collaborator Michael Mendillo (Boston University) will be Graduate Student’s academic advisor, which will ensure an active role for Mendillo. He will also advise on comparative aeronomy, including the terrestrial ionosphere and its response to solar flares (Mendillo and Evans, 1974; Mendillo et al., 1974). As stated in their letters of commitment, the collaborators’ levels of effort will be sufficient to fulfill their responsibilities. Collaborators will be invited to Boston for several days each year with travel funds supplied by BU’s Center for Space Physics.

References

- Blelly, P.-L., Lilensten, J., Robineau, A., Fontanari, J., and Alcayde, D. (1996) Calibration of a numerical ionospheric model with EISCAT observations, *Ann. Geophys.*, 14, 1375-1390.
- Bougher, S., Engel, S., Hinson, D., and Forbes, J. (2001) Mars Global Surveyor radio science electron density profiles: Neutral atmosphere implications, *Geophys. Res. Lett.*, 28, 3091-3094.
- Bougher, S. W., Roble, R. G., and Fuller-Rowell, T. (2002) Simulations of the upper atmospheres of the terrestrial planets, in *Atmospheres in the Solar System: Comparative Aeronomy*, *Geophys. Monogr. Ser.*, 130, eds. M. Mendillo, A. Nagy, J. H. Waite, AGU, Washington, DC.
- Bougher, S. W., Engel, S., Hinson, D. P., and Murphy, J. R. (2004) MGS Radio Science electron density profiles: Interannual variability and implications for the martian neutral atmosphere, *J. Geophys. Res.*, 109, E03010, doi:10.1029/2003JE002154.
- Bougher, S. W., Bell, J. M., Murphy, J. R., Lopez-Valverde, M. A., and Withers, P. (2006) Polar warming in the Mars thermosphere: Seasonal variations owing to changing insolation and dust distributions, *Geophys. Res. Lett.*, 33, L02203, doi:10.1029/2005GL024059.
- Breus, T. K., Krymskii, A. M., Crider, D. H., Ness, N. F., Hinson, D., and Barashyan, K. K. (2004) Effect of the solar radiation in the topside atmosphere/ionosphere of Mars: Mars Global Surveyor observations, *J. Geophys. Res.*, 109, A09310, doi:10.1029/2004JA010431.
- Chamberlin, P. C., Woods, T. N., and Eparvier, F. G. (2004) Flare Irradiance Spectral Model (FISM) A model of solar vacuum ultraviolet irradiance over timescales from flares to solar cycles, Fall AGU meeting, abstract #SM13B-02.
- Chamberlin, P. C. (2005) The Flare Irradiance Spectral Model (FISM). PhD dissertation, University of Colorado, available online at ftp://lasftp.colorado.edu/pub/SEE_Data/fism
- Chamberlin, P. C., Woods, T. N., and Eparvier, F. G. (2005a) First results from the Flare Irradiance Spectral Model (FISM): A model of solar vacuum ultraviolet irradiance over timescales from flares to solar cycles, Spring AGU meeting, abstract #SA23A-12.
- Chamberlin, P. C., Woods, T. N., and Eparvier, F. G. (2005b) Comparisons of new Flare Irradiance Spectral Model (FISM) to current solar ultraviolet irradiance measurements, Fall AGU meeting, abstract #SA34A-08.

Chamberlin, P. C., Woods, T. N., and Eparvier, F. G. (2007) Flare Irradiance Spectral Model (FISM): Daily component algorithms and results, *Space Weather*, 5, S07005, doi:10.1029/2007SW000316.

Chen, R. H., Cravens, T. E., and Nagy, A. F. (1978) The martian ionosphere in light of the Viking observations, *J. Geophys. Res.*, 83, 3871-3876.

Choi, Y. W., Kim, J., Min, K. W., Nagy, A. F., and Oyama, K. I. (1998) Effect of the magnetic field on the energetics of Mars ionosphere, *Geophys. Res. Lett.*, 25, 2753-2756.

Espley, J. R., Farrell, W. M., Brain, D. A., Morgan, D. D., Cantor, B., Plaut, J. J., Acuña, M. H., Picardi, G. (2007) Absorption of MARSIS radar signals: Solar energetic particles and the daytime ionosphere, *Geophys. Res. Lett.*, 34, L09101, doi:10.1029/2006GL028829.

Fox, J. L., and Delgarno, A. (1979) Ionization, luminosity, and heating of the upper atmosphere of Mars, *J. Geophys. Res.*, 84, 7315-7333.

Fox, J. L., Zhou, P., and Bougher, S. W. (1996) The Martian Thermosphere/Ionosphere at High and Low Solar Activities, *Adv. Space Res.*, 17(11) 203-218.

Fox, J. L. (2004) Response of the martian thermosphere/ionosphere to enhanced fluxes of solar X-rays, *J. Geophys. Res.*, 109, A11310, doi:10.1029/2004JA010380.

Fox, J. L., and Yeager, K. E. (2006) Morphology of the near-terminator martian ionosphere: A comparison of models and data, *J. Geophys. Res.*, 111, A10309, doi:10.1029/2006JA011697.

Fox, J. L. (2007) Near-terminator Venus ionosphere: How Chapman-esque?, *J. Geophys. Res.*, 112, E04S02, doi:10.1029/2006JE002736.

Galand, M., Lilensten, J., Kofman, W., Sidje, R. B. (1997) Proton transport model in the ionosphere 1. Multistream approach of the transport equations, *J. Geophys. Res.*, 102, 22261-22272.

Galand, M., Lilensten, J., Toubanc, D., and Maurice, S. (1999) The ionosphere of Titan: Ideal diurnal and nocturnal cases, *Icarus*, 140, 92-105.

Galand, M., Yelle, R. V., Coates, A. J., Backes, H., and Wahlund, J.-E. (2006) Electron temperature of Titan's sunlit ionosphere, *Geophys. Res. Lett.*, 33, L21101, doi:10.1029/2006GL027488.

GOES (2006) <http://goes.ngdc.noaa.gov/data/>

Gurnett, D. A., Kirchner, D. L., Huff, R. L., Morgan, D. D., Persoon, A. M., Averkamp, T. F., Duru, F., Nielsen, E., Safaeinili, A., Plaut, J. J., Picardi, G. (2005) Radar soundings of the ionosphere of Mars. *Science*, 310, 1929-1933.

Haider, S. A., Seth, S. P., Choksi, V. R., and Oyama, K. I. (2006) Model of photoelectron impact ionization within the high latitude ionosphere at Mars: Comparison of calculated and measured electron density, *Icarus*, 185, 102-112.

Hanson, W. B., Sanatani, S., and Zuccaro, D. R. (1977) The martian ionosphere as observed by the Viking Retarding Potential Analyzer, *J. Geophys. Res.*, 82, 4351-4363.

Hanson, W. B., and Mantas, G. P. (1988) Viking electron temperature measurements - evidence for a magnetic field in the martian ionosphere, *J. Geophys. Res.*, 93, 7538-7544.

Hantsch, M. H., and Bauer, S. J. (1990) Solar control of the Mars ionosphere, *Planet. Space Sci.*, 38, 539-542.

Kim, J., Nagy, A. F., Cravens, T. E., and Kliore, A. J. (1989) Solar cycle variations of the electron densities near the ionospheric peak of Venus, *J. Geophys. Res.*, 94, 11997-12002.

Krasnopolsky, V. A. (2002) Mars' upper atmosphere and ionosphere at low, medium, and high solar activities: Implications for evolution of water, *J. Geophys. Res.*, 107, E12, 5128, doi:10.1029/2001JE001809.

Krymskii, A. M., Ness, N. F., Crider, D. H., Breus, T. K., Acuna, M. H., and Hinson, D. P. (2004) Solar wind interaction with the ionosphere/atmosphere and crustal magnetic fields at Mars: Mars Global Surveyor Magnetometer/Electron Reflectometer, radio science, and accelerometer data, *J. Geophys. Res.*, 109, A11306, doi:10.1029/2004JA010420.

Liemohn, M. W., Ma, Y., Frahm, R. A., Xiaohua, F., Kozyra, J. U., Nagy, A. F., Winningham, J. D., Sharber, J. R., Barabash, S., Lundin, R. (2006) Mars global MHD predictions of magnetic connectivity between the dayside ionosphere and the magnetospheric flanks, *Space Sci. Rev.*, 126, 63-76.

Lilensten, J., Kofman, W., Wisenberg, J., Oran, E. S., and Devore, C. R. (1989) Ionization efficiency due to primary and secondary photoelectrons: A numerical model, *Ann. Geophys.*, 7, 83-90.

Lilensten, J., Simon, C., Witasse, O., Dutuit, O., Thissen, R., and Alcaraz, C. (2005) A fast computation of the diurnal secondary ion production in the ionosphere of Titan, *Icarus*, 174, 285-288.

Lummerzheim, D., and Lilensten, J. (1994) Electron transport and energy degradation in the ionosphere: Evaluation of the numerical solution, comparison with laboratory experiments and auroral observations, *Ann. Geophys.*, 12, 1039-1051.

LWS TRT SDT (2003) Living With a Star Targeted Research and Technology Science Definition Team Report, November 2003, http://lws-trt.gsfc.nasa.gov/TRT_SDT_Report.pdf

LWS TRT Town Hall Meeting Report (2006) http://lws-trt.gsfc.nasa.gov/lwstrt_AGUTownMtg.pdf

LWS TRT Steering Committee Report (2007) http://lws-trt.gsfc.nasa.gov/TRT_SC07report.pdf

Ma, Y., Nagy, A. F., Hansen, K. C., DeZeeuw, D. L., and Gombosi, T. I. (2002) Three-dimensional multispecies MHD studies of the solar wind interaction with Mars in the presence of crustal fields, *J. Geophys. Res.*, 107, doi:10.1029/2002JA009293.

Ma, Y., Nagy, A. F., Sokolov, I. V., and Hansen, K. C. (2004) Three-dimensional, multispecies, high spatial resolution MHD studies of the solar wind interaction with Mars, *J. Geophys. Res.*, 109, A07211, doi:10.1029/2003JA010367.

Martinis, C. R., Wilson, J. K., and Mendillo, M. (2003) Modeling day-to-day ionospheric variability on Mars, *J. Geophys. Res.*, 108, A10, 1383, doi:10.1029/2003JA009973.

Mendillo, M., and Evans, J. V. (1974) Incoherent scatter observations of the ionospheric response to a large solar flare, *Radio Sci.*, 9, 197-203.

Mendillo, M., and 14 colleagues (1974) Behavior of the ionospheric F-region during the great solar flare of August 7, 1972, *J. Geophys. Res.*, 79, 665-672.

Mendillo, M., Smith, S. M., Wilson, J. K., Rishbeth, H., and Hinson, D. P. (2003) Simultaneous ionospheric variability on Earth and Mars, *J. Geophys. Res.*, 108, doi:10.1029/2003JA009961.

Mendillo, M., Pi, X., Smith, S. M., Martinis, C., Wilson, J., and Hinson, D. (2004) Ionospheric effects upon a satellite navigation system at Mars, *Radio Sci.*, 39, RS2028, doi:10.1029/2003RS002933.

Mendillo, M., Withers, P., Hinson, D., Rishbeth, H., and Reinisch, B. (2006) Effects of solar flares on the ionosphere of Mars, *Science*, 311, 1135-1138.

Mendillo, M., and Withers, P. (2006) Effects of solar flares on Earth and Mars, Spring AGU meeting, abstract U52A-02.

Mitchell, D. L., Lin, R. P., Rème, H., Crider, D. H., Cloutier, P. A., Connerney, J. E. P., Acuña, M. H., and Ness, N. F. (2000) Oxygen Auger electrons observed in Mars' ionosphere, *Geophys. Res. Lett.*, 27, 1871-1874.

Molina-Cuberos, G. J., Lichtenegger, H., Schwinenschuh, K., Lopez-Moreno, J. J., and Rodrigo, R. (2002) Ion-neutral chemistry model of the lower ionosphere of Mars, *J. Geophys. Res.*, 107, E55027, doi:10.1029/2000JE001447.

Molina-Cuberos, G. J., Witasse, O., Lebtrein, J.-P., Rodrigo, R., and Lopez-Moreno, J. J. (2003) Meteoric ions in the atmosphere of Mars, *Planet. Space Sci.*, 51, 239-249.

Morgan, D. D., Gurnett, D. A., Kirchner, D. L., Huff, R. L., Brain, D. A., Boynton, W. V., Acuña, M. H., Plaut, J. J., and Picardi, G. (2006) Solar control of radar wave absorption by the martian ionosphere, *Geophys. Res. Lett.*, 33, L13202, doi:10.1029/2006GL026637

Neupert, W. M. (2006) Variability of the solar soft X-ray irradiance (0.6-2.5 nm) with solar activity, *Adv. Space Res.*, 37, 238-245.

Nielsen, E., Zou, H., Gurnett, D. A., Kirchner, D. L., Morgan, D. D., Huff, R., Orosei, R., Safaenili, Plaut, J. J., and Picardi, G. (2006) Observations of vertical reflections from the topside martian ionosphere, *Space Sci. Rev.*, 126, 373-388.

Nielsen, E., Morgan, D. D., Kirchner, D. L., Plaut, J., and Picardi, G. (2007) Absorption and reflection of radio waves in the martian ionosphere, *Planet. Space Sci.*, 55, 864-870.

Patzold, M., Tellman, S., Hausler, B., Hinson, D., Schaa, R., and Tyler, G. L. (2005) A sporadic third layer in the ionosphere of Mars, *Science*, 310, 837-839.

Pesnell, W. D., and Grebowsky, J. (2000) Meteoric magnesium ions in the martian atmosphere, *J. Geophys. Res.*, 105, 1695-1707.

Rees, M. H., and Jones, A. V. (1973) Time dependent studies of the aurora 2. Spectroscopic morphology, *Planet. Space Sci.*, 21, 1213-1235.

Richards, P. G., and Torr, D. G. (1988) Ratios of photoelectron to EUV ionization rates for aeronomic studies, *J. Geophys. Res.*, 93, 4060-4066.

Rishbeth, H., and Garriott, O. K. (1969) *Introduction to Ionospheric Physics*, Academic Press.

Rishbeth, H., and Mendillo, M. (2004) Ionospheric layers of Mars and Earth, *Planet. Space Sci.*, 52, 849-852, 2004.

ROSES (2007) ROSES NASA Research Announcement

Schunk, R., and Nagy, A., (2000) *Ionospheres: Physics, Plasma Physics, and Chemistry*, Camb. Univ. Press., NY.

Shinagawa, H., and Cravens, T. E. (1989) A one-dimensional multispecies magnetohydrodynamic model of the dayside ionosphere of Mars, *J. Geophys. Res.*, 94, 6506-6516.

Shinagawa, H., and Cravens, T. E. (1992) The ionospheric effects of a weak intrinsic magnetic field at Mars, *J. Geophys. Res.*, 97, 1027-1035.

Simon, C., Witasse, O., Leblanc, F., Lilensten, J., Mouginot, J., Kofman, W., and Bertaux, J.-L. (2007) Analysis and modelling of SPICAM data onboard Mars Express, EGU meeting, EGU2007A-06650.

Sutton, E. K., Forbes, J. M., Nerem, R. S., and T. N. Woods (2006) Neutral density response to the solar flares of October and November, 2003, *Geophys. Res. Lett.*, 33, L22101, doi:10.1029/2006GL027737.

Titheridge, J. E. (1996) Direct allowance for the effect of photoelectrons in ionospheric modeling, *J. Geophys. Res.*, 101, 357-369.

Tobiska, W. K., Woods, T., Eparvier, F., Viereck, R., Floyd, L., Bouwer, D., Rottman, G., and White, O. R. (2000) The SOLAR2000 empirical solar irradiance model and forecast tool, *J. Atmos. And Solar-Terr. Phys.*, 62, 1233-1250.

Tobiska, W. K. (2004) SOLAR2000 irradiances for climate change research, aeronomy, space systems engineering, *Adv. Space Res.*, 34, 1736-1746.

Verner, D. A., and Yakovlev, D. G. (1995) Analytic fits for partial photoionization cross sections, *Astronomy and Astrophysics Supplement Series*, 109, 125-133.

Verner, D. A., Ferland, G. J., Korista, K. T., and Yakovlev, D. G. (1996) Atomic data for astrophysics II. New analytic fits for photoionization cross sections of atoms and ions, *Astrophys. J.*, 465, 487-498.

Whitten, R. C., Poppoff, I. G., and Sims, J. S. (1971) The ionosphere of Mars below 80 km altitude, *Planet. Space Sci.*, 17, 243-250.

Witasse, O., Blelly, P.-L., Lilensten, J., Leblanc, F. (2006) TRANSMARS, a kinetic-fluid model of the martian ionosphere, European Planetary Science Congress, EPSC2006-A-00011.

Withers, P., Bougher, S. W., and Keating, G. M. (2003) The effects of topographically-controlled thermal tides on the martian upper atmosphere as seen by the MGS accelerometer, *Icarus*, 164, 14-32.

Withers, P., Mendillo, M., Rishbeth, H., Hinson, D. P., and Arkani-Hamed, J. (2005) Ionospheric characteristics above martian crustal magnetic anomalies, *Geophys. Res. Lett.*, 32, L16204, doi:10.1029/2005GL023483.

Withers, P., and Mendillo, M. (2005) Response of peak electron densities in the martian ionosphere to day-to-day changes in solar flux due to solar rotation, *Planet. and Space Sci.*, 53, 1401-1418.

Withers, P. (2006) Mars Global Surveyor and Mars Odyssey accelerometer observations of the martian upper atmosphere during aerobraking, *Geophys. Res. Lett.*, 33, L02201, doi:10.1029/2005GL024447.

Withers, P., Wroten, J., Mendillo, M., Chamberlin, P., and Woods, T. (2007a) Modeling the effects of solar flares on the ionosphere of Mars, European Geophysical Union Annual Meeting, abstract EG2007-A-05089.

Withers, P., Wroten, J., Mendillo, M., and Chamberlin, P. (2007b) Simulations of the Mars ionosphere during a solar flare, Spring AGU Meeting, abstract SA31B-05.

Biographical Sketch for PI Paul Withers

Center for Space Physics
Boston University
725 Commonwealth Avenue
Boston MA 02215

Tel: (617) 353 1531
Fax: (617) 353 6463
Email: withers@bu.edu
Citizenship: British

Education

- PhD, Planetary Science, University of Arizona 2003
- MS, Physics, Cambridge University, Great Britain 1998
- BA, Physics, Cambridge University, Great Britain 1998

Recent Professional Experience

- Research associate Dr. Michael Mendillo (Boston Univ) 2003-present
Analysis of ionospheric data from Mars and Earth, plus numerical modelling
- Graduate research assistant Dr. Stephen Bougher (Univ. of Arizona) 1998 – 2003
Studied weather in the martian upper atmosphere. Played an advisory role in mission operations for Mars Global Surveyor and Mars Odyssey aerobraking

Fellowships, Honors, and Awards

- CEDAR Postdoctoral Fellowship from NSF for upper atmospheric research 2003
- Kuiper Memorial Award from the University of Arizona for excellence 2002
in academic work and research in planetary science.

Selected Peer Reviewed Publications and Other Major Publications

- Crosby, Bothmer, Facius, Griessmeier, Moussas, Panasyuk, Romanova, and **Withers** “Interplanetary Space Weather and its Planetary Connection” (2007) *Space Weather*, under review.
- Christou, Vaubaillon, and **Withers** “The dust trail complex of comet 79P/du Toit-Hartley and meteor outbursts at Mars” (2007) *Astronomy and Astrophysics*, in press.
- **Withers** “A technique to determine the mean molecular mass of a planetary atmosphere using pressure and temperature measurements made by an entry probe: Demonstration using Huygens data” (2007) *Planetary and Space Science*, 55, in press, 10.1016/j.pss.2007.04.009.
- Montabone, Lewis, Read, and **Withers** “Reconstructing the weather on Mars at the time of the MERs and Beagle 2 landings” (2006) *Geophysical Research Letters*, 33, L19202, doi:10.1029/2006GL026565.
- **Withers** and Smith “Atmospheric entry profiles from the Mars Exploration Rovers Spirit and Opportunity” (2006) *Icarus*, 185, 133-142, doi:10.1016/j.icarus.2006.06.013.
- Mendillo, **Withers**, Hinson, Rishbeth, and Reinisch “Effects of solar flares on the ionosphere of Mars” (2006) *Science*, 311, 1135-1138.

- Bougher and 4 colleagues, including **Withers** “Polar warming in in the Mars thermosphere: Seasonal variations owing to changing insolation and dust distributions” (2006) *Geophysical Research Letters*, 33, L02203, doi:10.1029/2005GL024059.
- **Withers** “Mars Global Surveyor and Mars Odyssey Accelerometer observations of the martian upper atmosphere during aerobraking” (2006) *Geophysical Research Letters*, 33, L02201, doi:10.1029/2005GL024447.
- Fulchignoni and 42 colleagues, including **Withers** “In situ measurements of the physical characteristics of Titan's environment” (2005), *Nature*, **438**, 785-791, doi:10.1038/nature04314.
- **Withers** and Mendillo “Response of peak electron densities in the martian ionosphere to day-to-day changes in solar flux due to solar rotation” (2005) *Planetary and Space Science*, **53**, 1401-1418, doi:10.1016/j.pss.2005.07.010.
- **Withers** “What is a planet?” (2005) *Eos*, **86**(36), 326, doi:10.1029/2005EO360004.
- **Withers**, Mendillo, Rishbeth, Hinson, and Arkani-Hamed “Ionospheric characteristics above Martian crustal magnetic anomalies” (2005) *Geophysical Research Letters*, **32**, L16204, doi:10.1029/2005GL023483.
- **Withers**, Bougher, and Keating, “The Effects of Topographically-Controlled Thermal Tides in the Martian Upper Atmosphere as seen by the MGS Accelerometer”, (2003) *Icarus*, **164**, 14-32.
- **Withers**, Towner, Hathi, and Zarnecki, “Analysis of entry accelerometer data: A case study of Mars Pathfinder”, (2003) *Planetary and Space Science*, **51**, 541-561.
- **Withers** and Neumann, “Enigmatic northern plains of Mars” (2001) *Nature*, **410**, 651.
- **Withers**, “Meteor storm evidence against the recent formation of lunar crater Giordano Bruno” (2001) *Meteoritics and Planetary Science*, **36**, 525 – 529.

Professional Activities and Service

- Reviewer of MER, MRO, Huygens, and Rosetta for NASA PDS and ESA 2004 - present
- Review panel member for NASA Mars Data Analysis Program, NASA Planetary Atmospheres Program, NASA Venus Express Participating Scientist Program, NASA Mars Fundamental Research program, NSF Astronomy and Astrophysics Research Grants Program 2004 - present
- Reviewer for Advances in Space Research, Annales Geophysicae, Icarus, Journal of Geophysical Research, Journal of Spacecraft and Rockets, Mars, Meteoritics and Planetary Science, Planetary and Space Science, and Science. 2001 - present
- Funded co-investigator on NASA Mars Scout Phase A grant for “The Great Escape” mission 2007
- Huygens SSP and HASI/ACC Team Member 2005 - present
- NASA 2003 Mars Exploration Rovers – Atmospheric Advisory Team. 2002 – 2004
- Beagle 2 Environmental Sensor Suite Team Member 2001 - 2003

Professional Affiliations: Member of the American Geophysical Union’s Planetary Sciences Section, the American Astronomical Society’s Division for Planetary Science, and the British Planetary Forum.